



## 1 **A proxy for atmospheric daytime gaseous sulfuric acid** 2 **concentration in urban Beijing**

3 Yiqun Lu<sup>1</sup>, Chao Yan<sup>2</sup>, Yueyun Fu<sup>3</sup>, Yan Chen<sup>4</sup>, Yiliang Liu<sup>1</sup>, Gan Yang<sup>1</sup>, Yuwei Wang<sup>1</sup>,  
4 Federico Bianchi<sup>2</sup>, Biwu Chu<sup>2</sup>, Ying Zhou<sup>5</sup>, Rujing Yin<sup>3</sup>, Rima Baalbaki<sup>2</sup>, Olga Garmash<sup>2</sup>,  
5 Chenjuan Deng<sup>3</sup>, Weigang Wang<sup>4</sup>, Yongchun Liu<sup>5</sup>, Tuukka Petäjä<sup>2,5,6</sup>, Veli-Matti Kerminen<sup>2</sup>,  
6 Jingkun Jiang<sup>3</sup>, Markku Kulmala<sup>2,5</sup>, Lin Wang<sup>1,7,8\*</sup>

7 <sup>1</sup> Shanghai Key Laboratory of Atmospheric Particle Pollution and Prevention (LAP<sup>3</sup>),  
8 Department of Environmental Science & Engineering, Jiangwan Campus, Fudan University,  
9 Shanghai 200438, China

10 <sup>2</sup> Institute for Atmospheric and Earth System Research / Physics, Faculty of Science, University  
11 of Helsinki, 00014 Helsinki, Finland

12 <sup>3</sup> State Key Joint Laboratory of Environment Simulation and Pollution Control, School of  
13 Environment, Tsinghua University, Beijing 100084, China

14 <sup>4</sup> Institute of Chemistry, Chinese Academy of Sciences, Beijing 100190, China

15 <sup>5</sup> Aerosol and Haze Laboratory, Advanced Innovation Center for Soft Matter Science and  
16 Engineering, Beijing University of Chemical Technology, Beijing 100029, China

17 <sup>6</sup> Joint International Research Laboratory of Atmospheric and Earth System Sciences  
18 (JirLATEST), School of Atmospheric Sciences, Nanjing University, Nanjing 210023, China

19 <sup>7</sup> Institute of Atmospheric Sciences, Jiangwan Campus, Fudan University, Shanghai 200438,  
20 China

21 <sup>8</sup> Shanghai Institute of Pollution Control and Ecological Security, Shanghai 200092, China

22 \* *Corresponding Author: L.W., email, [lin\\_wang@fudan.edu.cn](mailto:lin_wang@fudan.edu.cn); phone, +86-21-31243568.*

23

24 **Abstract.** Gaseous sulfuric acid is known as one of the key precursors for atmospheric  
25 new particle formation processes, but its measurement remains a major challenge. A  
26 proxy method that is able to derive gaseous sulfuric acid concentrations from  
27 parameters that can be measured relatively easily and accurately is therefore highly  
28 desirable among the atmospheric chemistry community. Although such methods are  
29 available for clean atmospheric environments, a proxy that works well in a polluted  
30 atmosphere, such as those in Chinese megacities, is yet to be developed. In this study,  
31 the gaseous sulfuric acid concentration was measured in February-March, 2018, in  
32 urban Beijing by a nitrate based - Long Time-of-Flight Chemical Ionization Mass  
33 Spectrometer (LToF-CIMS). A number of atmospheric parameters were recorded  
34 concurrently including the ultraviolet radiation B (UVB) intensity, concentrations of O<sub>3</sub>,  
35 NO<sub>x</sub>, SO<sub>2</sub> and HONO, and aerosol particle number size distributions. A proxy for  
36 atmospheric daytime gaseous sulfuric acid concentration was derived using a statistical



37 analysis method by using the UVB intensity, [SO<sub>2</sub>], condensation sink (CS), [O<sub>3</sub>], and  
38 [HONO] (or [NO<sub>x</sub>]) as the predictor variables. In this proxy method, we considered the  
39 formation of gaseous sulfuric acid from reactions of SO<sub>2</sub> and OH radicals during the  
40 daytime, and loss of gaseous sulfuric acid due to its condensation onto the pre-existing  
41 particles. In addition, we explored formation of OH radicals from the conventional gas-  
42 phase photochemistry using ozone as a proxy and from the photolysis of  
43 heterogeneously-formed HONO using HONO (and subsequently NO<sub>x</sub>) as a proxy. Our  
44 results showed that the UVB intensity and [SO<sub>2</sub>] are dominant factors for the production  
45 of gaseous sulfuric acid, and that the simplest proxy could be constructed with the UVB  
46 intensity and [SO<sub>2</sub>] alone, resulting in up to 29% relative deviations when sulfuric acid  
47 concentrations were larger than  $2.0 \times 10^6$  molecules cm<sup>-3</sup>. When the OH radical  
48 production from both homogeneously- and heterogeneously-formed precursors were  
49 considered, the relative deviations were lower than 24%.



## 50 **1 Introduction**

51 Gaseous sulfuric acid ( $\text{H}_2\text{SO}_4$ ) is a key precursor for atmospheric new particle  
52 formation (NPF) processes (Kerminen, 2018; Kirkby et al., 2011; Kuang et al., 2008;  
53 Kulmala and Kerminen, 2008; Sipilä et al., 2010). A number of atmospheric nucleation  
54 mechanisms including  $\text{H}_2\text{SO}_4\text{-H}_2\text{O}$  binary nucleation (Benson et al., 2008; Duplissy et  
55 al., 2016; Kirkby et al., 2011),  $\text{H}_2\text{SO}_4\text{-NH}_3\text{-H}_2\text{O}$  ternary nucleation (Kirkby et al., 2011;  
56 Korhonen et al., 1999; Kürten et al., 2015), and  $\text{H}_2\text{SO}_4\text{-DMA-H}_2\text{O}$  ternary nucleation  
57 (Almeida et al., 2013; Petäjä et al., 2011; Yao et al., 2018) demand the participation of  
58 gaseous sulfuric acid molecules. In addition, the condensation of gaseous sulfuric acid  
59 onto newly-formed particles contributes to their initial growth (Kulmala et al., 2013).  
60 Quantitative assessments of the contribution of gaseous sulfuric acid to both the new  
61 particle formation rates and the particle growth rates require real-time measurements of  
62 gaseous sulfuric acid concentrations during the NPF events (Nieminen et al., 2010;  
63 Paasonen et al., 2010).

64 Measurements of gaseous sulfuric acid in the lower troposphere are challenging  
65 because its ambient concentration is typically quite low ( $10^6\text{-}10^7$  molecule  $\text{cm}^{-3}$ )  
66 (Kerminen et al., 2010; Mikkonen et al., 2011). Reported real-time measurements of  
67 gaseous sulfuric acid are currently based on Chemical Ionization Mass Spectrometry  
68 with  $\text{NO}_3^-$  as reagent ions (nitrate CIMS) because CIMS has a low detection limit for  
69 the atmospheric concentration range of gaseous sulfuric acid (Jokinen et al., 2012), and  
70 a constant fraction of sulfuric acid present in the air sample will be ionized by excessive  
71 nitrate ions in CIMS under constant instrumental conditions (Kürten et al., 2012; Zheng  
72 et al., 2010), which makes the quantification of gaseous sulfuric acid feasible.

73 Arnold and Fabian (1980) measured the negative ions in the stratosphere using a  
74 passive CIMS and derived the concentration of stratospheric gaseous sulfuric acid from  
75 the fractional abundances of a series of stratospheric negative ions as well as the  
76 associated equilibrium or rate constants. Later, real-time measurement of sulfuric acid  
77 in the lower troposphere was performed using nitrate CIMS (Eisele and Tanner, 1993),  
78 with laboratory calibrations by production of known concentrations of OH radicals that  
79 will be titrated into gaseous sulfuric acid. Thereafter, measurements of sulfuric acid  
80 using CIMS have been performed around the world (e.g., Berresheim et al., 2000;  
81 Bianchi et al., 2016; Jokinen et al., 2012; Kuang et al., 2008; Kürten et al., 2014; Kurtén  
82 et al., 2011; Petäjä et al., 2009; Weber et al., 1997; Zheng et al., 2011), and CIMS has  
83 been proved to be a robust tool for gaseous sulfuric acid detection. However, sulfuric



84 acid measurements are still rather sparse because of the high cost of the CIMS  
85 instrument and the extensive demand of specialized expertise on the instrument  
86 calibration, maintenance, and data processing, etc. Therefore, a proxy for gaseous  
87 sulfuric acid concentration is highly desirable.

88 Proxies for the estimation of atmospheric gaseous sulfuric acid concentrations  
89 were previously developed to approximate measurement results of sulfuric acid  
90 in Hyytiälä, Southern Finland (Petäjä et al., 2009), supposing that gaseous sulfuric acid  
91 is formed from reactions between SO<sub>2</sub> and OH radicals, and lost due to its condensation  
92 onto pre-existing particles. The derived simplest proxy can be written as Eq. (1) below,  
93 and the authors recognized that the proxies might be site-specific and should be verified  
94 prior to utilization in other environments.

95

$$96 \quad [H_2SO_4] = k \cdot \frac{[SO_2] \cdot (UVB \text{ or } Global \text{ radiation})}{CS} \quad (1)$$

97

98 Mikkonen et al. (2011) later developed a couple of statistical proxies based on  
99 measurements of sulfuric acid in six European and North American sites, including  
100 urban, rural and forest areas. Their results showed that the radiation intensity and [SO<sub>2</sub>]  
101 are the most important factors to determine the concentration of sulfuric acid, and that  
102 the impact of condensation sink (CS), a proxy for condensational sink for gaseous  
103 sulfuric acid, is generally negligible. In several proxies developed by Mikkonen et al.  
104 (2011), the correlation between the gaseous sulfuric acid concentration and CS is  
105 positive, which is against what one would expect. In addition, the performance of a  
106 proxy equation is site-specific because of varying atmospheric conditions from one site  
107 to another, which implies that the proxy suggested by Mikkonen et al. (2011) might not  
108 work well in locations that characterized with an atmospheric environment different  
109 from those in the six sites of that study.

110 Beijing is a location with typical values of CS being 10-100 times higher  
111 (Herrmann et al., 2014; Wu et al., 2007; Xiao et al., 2015; Yue et al., 2009; Zhang et al.,  
112 2011) and typical SO<sub>2</sub> concentrations being 1-10 times higher (Wang et al., 2011a; Wu  
113 et al., 2017) than those in Europe and North America (Mikkonen et al., 2011), yet  
114 measured gaseous sulfuric acid concentrations are relatively similar between these  
115 environments (Wang et al., 2011b; Zheng et al., 2011). Whether previous proxies  
116 developed for European and North American sites work in Beijing remains to be tested.



117 Furthermore, in addition to the gas phase reaction between O(<sup>1</sup>D) and water molecules  
118 (Crutzen and Zimmermann, 1991; Logan et al., 1981), photolysis of HONO could be a  
119 potentially important source of OH radical in the atmosphere not only in the early  
120 morning (Alicke et al., 2002, 2003; Elshorbany et al., 2009; Li et al., 2012) but also  
121 during the daytime (Acker et al., 2005; Aumont et al., 2003; Kleffmann, 2007). An  
122 experimental study measuring HONO near the surface layer estimated that HONO was  
123 a main contributor to OH production in Beijing, with HONO's contribution being larger  
124 than 70% at around 12:00-13:00, except for summer when the contribution of O<sub>3</sub>  
125 dominated (Hendrick et al., 2014). Given the distinct characteristics of these two OH  
126 radical formation pathways, they both should be included and evaluated separately  
127 when a proxy for atmospheric gaseous sulfuric acid concentration is being built. The  
128 reactions between SO<sub>2</sub> and criegee intermediates formed from the ozonolysis of  
129 atmospheric alkenes could be a potential source of sulfuric acid only in the absence of  
130 solar radiation (Boy et al., 2013; Mauldin et al., 2012), so these reactions are expected  
131 to provide a minor contribution to the formation of gaseous sulfuric acid during the  
132 daytime in urban Beijing.

133 In this study, gaseous sulfuric acid concentration was measured by a Long Time-  
134 of-Flight Chemical Ionization Mass Spectrometer (LToF-CIMS) in February - March,  
135 2018, in urban Beijing. A number of atmospheric parameters were recorded  
136 concurrently, including the ultraviolet radiation B (UVB) intensity, concentrations of  
137 O<sub>3</sub>, NO<sub>x</sub>, SO<sub>2</sub> and HONO, and particle number size distributions. The objective of this  
138 study is to develop a robust daytime gaseous sulfuric acid concentration proxy for  
139 Beijing, a representative Chinese megacity with urban atmospheric environments.

140

## 141 **2 Ambient measurements**

142 An intensive campaign was carried out from 9 February to 14 March, 2018 on the  
143 fifth floor of a teaching building in the west campus of Beijing University of Chemical  
144 Technology (39° 94' N, 116° 30' E). This monitoring site is 2 km to the west of the West  
145 3<sup>rd</sup> Ring Road and surrounded by commercial properties and residential dwellings.  
146 Hence, this station can be regarded as a representative urban site.

147 The sulfuric acid concentration was measured by a LToF-CIMS (Aerodyne  
148 Research, Inc.) equipped with a nitrate chemical ionization source. Ambient air was  
149 drawn into the ionization source through a stainless-steel tube with a length of 1.6 m  
150 and a diameter of 3/4 inch. A mixture of a 3 standard cubic centimeter per minute (scm)



151 ultrahigh purity nitrogen flow containing nitric acid and a 20 standard liter per minute  
152 (slpm) pure air flow supplied by a zero-air generator (Aadco 737, USA), together as a  
153 sheath flow, was guided through a PhotoIonizer (Model L9491, Hamamatsu, Japan) to  
154 produce nitrate reagent ions. This sheath flow was then introduced into a co-axial  
155 laminar flow reactor concentric to the sample flow. Nitrate ions were pushed to the  
156 middle of sample flow under an electric field and subsequently charged sample  
157 molecules. During the campaign, the sample flow rate was kept at 8.4 slpm, since mass  
158 flow controllers fixed the sheath flow rate and the excess flow rate and the flow into  
159 the mass spectrometer (around 0.4 slpm) was fixed by the size of a pinhole between the  
160 ionization source and the mass spectrometer. The CIMS was calibrated twice during  
161 the campaign following the protocols in previous literatures (Kürten et al., 2012; Zheng  
162 et al., 2015). Here we use  $1.1 \times 10^{10}$  molecule  $\text{cm}^{-3}$  as the calibration coefficient, after  
163 taking into account diffusion losses in the stainless-steel tube and the nitrate chemical  
164 ionization source. The obtained mass spectra were analyzed with a tofTools package  
165 based on the MATLAB software (Junninen et al., 2010).

166 Ambient particle number size distributions down to about 1 nm were measured  
167 using a combination of a scanning mobility particle sizer spectrometer (SMPS)  
168 equipped with a diethylene glycol-based condensation particle counter (DEG-CPC, ~1-  
169 10 nm) and a conventional particle size distribution system (PSD, ~3-700 nm)  
170 consisting of a pair of aerosol mobility spectrometers developed by Tsinghua  
171 University (Cai et al., 2017; Jiang et al., 2011; Liu et al., 2016). The values of CS were  
172 calculated following Eq. (2) (Dal Maso et al., 2002):

$$173 \quad CS = 2\pi D \int_0^{\infty} D_p \beta_m(D_p) n(D_p) dD_p = 2\pi D \sum_i \beta_i D_{pi} N_i \quad (2)$$

174 where  $D_{pi}$  is the geometric mean diameter of particles in the size bin  $i$  and  $N_i$  is the  
175 particle number concentration in the corresponding size bin.  $D$  is the diffusion  
176 coefficient of gaseous sulfuric acid, and  $\beta_m$  represents a transition-regime correction  
177 factor that could be defined as a function of the Knudsen number (Fuchs and Sutugin,  
178 1971).

179  $\text{SO}_2$ ,  $\text{O}_3$  and  $\text{NO}_x$  concentrations were measured using a  $\text{SO}_2$  analyzer (Model 43i,  
180 Thermo, USA), a  $\text{O}_3$  analyzer (Model 49i, Thermo, USA) and a  $\text{NO}_x$  analyzer (Model  
181 42i, Thermo, USA) with the detection limits of 0.1 ppbv, 0.5 ppbv and 0.4 ppbv,  
182 respectively. The above instruments were pre-calibrated before the campaign. The UVB  
183 (280 - 315 nm) intensity (UV-S-B-T, KIPP&ZONEN, The Netherlands) was measured



184 on the rooftop of the building. Atmospheric HONO concentrations were measured by  
185 a home-made HONO analyzer with a detection limit of 0.01 ppbv (Tong et al., 2016).

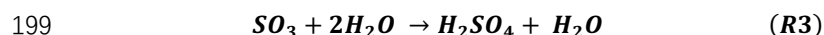
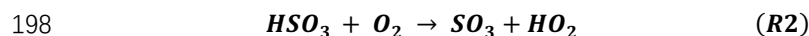
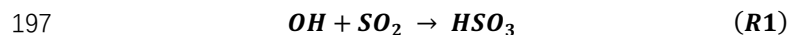
186 Particle number size distributions and concentrations of gaseous sulfuric acid, SO<sub>2</sub>,  
187 O<sub>3</sub>, NO<sub>2</sub> and HONO were recorded with a time resolution of 5 min, and the UVB  
188 intensity with time resolution of 1 min. A linear interpolation method was used for  
189 deriving the variables with the same time intervals, *i.e.*, 5 min. Only data between local  
190 sunrise and sunset were used in the subsequent analysis.

191

### 192 3 Development of a proxy for atmospheric gaseous sulfuric acid

193 We derived the gaseous sulfuric acid concentration proxy on the basis of currently  
194 accepted formation pathways of sulfuric acid in the atmosphere (R1-R3) (Finlayson-  
195 Pitts and Pitts, 2000; Stockwell and Calvert, 1983):

196



200

201 The reaction (R1) is the rate-limiting step of this formation pathway (Finlayson-Pitts  
202 and Pitts, 2000), so our proxy will consider the two major processes that determine the  
203 abundance of gaseous sulfuric acid: the formation of gaseous sulfuric acid from  
204 reactions between SO<sub>2</sub> and OH radicals, and the loss of gaseous sulfuric acid due to its  
205 condensation onto pre-existing particles (Dal Maso et al., 2002; Kulmala et al., 2012;  
206 Pirjola et al., 1999).

207 The rate of change of sulfuric acid concentration can be written as Eq. (3)  
208 (Mikkonen et al., 2011):

209

$$210 \quad \frac{d[\text{H}_2\text{SO}_4]}{dt} = k \cdot [\text{OH}] \cdot [\text{SO}_2] - [\text{H}_2\text{SO}_4] \cdot CS \quad (3)$$

211

212 where  $k$  is a temperature-dependent reaction constant (DeMore et al., 1997). To  
213 simplify the calculation, the production and loss of sulfuric acid can be assumed to be  
214 at pseudo steady-state (Mikkonen et al., 2011; Petäjä et al., 2009). Then the sulfuric  
215 acid concentration can be written as Eq. (4).

216

$$217 \quad [\text{H}_2\text{SO}_4] = k \cdot [\text{OH}] \cdot [\text{SO}_2] \cdot CS^{-1} \quad (4)$$



218 Atmospheric OH radical measurements represent a major challenge as well. Since  
219 previous studies suggest that the OH radical concentration is strongly correlated with  
220 the intensity of UVB, [OH] could be replaced with UVB intensity in the proxy equation  
221 (Petäjä et al., 2009; Rohrer and Berresheim, 2006). Although photolysis of O<sub>3</sub>  
222 ( $\lambda < 320 \text{ nm}$ ) and subsequent reactions with H<sub>2</sub>O are considered to be the dominant  
223 source of OH radicals in the atmosphere (Logan et al., 1981), recent studies argue that  
224 photolysis of HONO ( $\lambda < 400 \text{ nm}$ ) is a potentially important OH radical formation  
225 pathway (Hendrick et al., 2014; Kleffmann, 2007; Su et al., 2011; Villena et al., 2011).  
226 Thus, we attempt to introduce both O<sub>3</sub> and HONO into the proxy equation and evaluate  
227 their effects on the concentration of OH radicals.

228 In practice, the values of the exponential factors in nonlinear fitting procedures are  
229 rarely equal to 1 (Mikkonen et al., 2011), so we replaced the factors  $x_i$  with  $x_i^{w_i}$  in  
230 the proxy, where  $x_i$  can be an atmospheric variable and  $w_i$  defines  $x_i$ ' weight in the  
231 proxy. Since  $k$  is a temperature-dependent reaction constant and varies within a 10 %  
232 range (in the atmosphere temperature range of 267.6 - 292.6 K), we further replaced  $k$   
233 with a scaling factor  $k_0$  that is also used in the proxy methods built in Hyytiälä, Southern  
234 Finland (Petäjä et al., 2009). As a result, the general proxy equation can be written as  
235 Eq. (5), with the UVB intensity, [SO<sub>2</sub>], condensation sink (CS), [O<sub>3</sub>], and [HONO] (or  
236 [NO<sub>x</sub>]) as predictor variables:

237

$$238 \quad [H_2SO_4] = f(k_0, x_i^{w_i}), \quad x_i = UVB, [SO_2], CS, [O_3], [HONO] \dots \quad (5)$$

239

240 The nonlinear curve-fitting procedures using iterative least square estimation for  
241 the proxies of gaseous sulfuric acid concentration based on Eq. (4) were performed by  
242 a MATLAB software.

243

## 244 4 Results and discussion

### 245 4.1 General Characteristics of daytime sulfuric acid and atmospheric parameters

246 Table 1 summarizes the mean, median and 5-95 % percentiles of gaseous sulfuric  
247 acid concentrations and other variables measured during the daytime of the campaign.  
248 The 5-95 % percentile ranges of the UVB intensity, [SO<sub>2</sub>], [NO<sub>2</sub>] and [O<sub>3</sub>] were 0-0.45  
249 W m<sup>-2</sup>, 0.9-11.4 ppbv, 3.3-61.4 ppbv and 3.5-23.3 ppbv, respectively. Compared with  
250 the sites in the study by Mikkonen et al. (2011), Beijing was characterized with a factor  
251 of 1.4-13.1 higher mean [SO<sub>2</sub>] but a factor of 3.4-5.4 lower mean [O<sub>3</sub>]. The 5-95 %





252 percentile range of CS in Beijing was 0.01-0.24 s<sup>-1</sup>, which is about 1-2 orders of  
253 magnitude larger than corresponding value ranges in Europe and North America. The  
254 concentration of gaseous sulfuric acid during this campaign was (2.2 – 10.0) × 10<sup>6</sup>  
255 molecule cm<sup>-3</sup> was in a 5-95 % percentile range of, relatively similar to observed  
256 elsewhere around the world. A diurnal mean concentration of 0.74 ppbv for HONO was  
257 observed in this campaign, consistent with previous long-term HONO measurements  
258 of about 0.48-1.8 ppbv (averaged values) in winter in Beijing (Hendrick et al., 2014;  
259 Spataro et al., 2013; Wang et al., 2017), which is a factor of 4-10 higher than HONO  
260 concentrations measured in Europe (Alicke et al., 2002, 2003). In addition, Beijing is  
261 dry in winter with an ambient relative humidity generally lower than 60%.

262

#### 263 4.2 Correlations between [H<sub>2</sub>SO<sub>4</sub>] and atmospheric variables

264 Table 2 summarizes the correlation coefficients between [H<sub>2</sub>SO<sub>4</sub>] and atmospheric  
265 variables using a Spearman-type correlation analysis. Note that only correlations with  
266 p-values smaller than 0.01 were included to ensure a statistical significance. Clearly,  
267 the UVB intensity is an isolated variable that is independent of all the other variables  
268 but that imposes a positive influence on O<sub>3</sub> because of photochemical formation of  
269 ozone, and a negative influence on HONO because of HONO's photochemical  
270 degradation. The sulfuric acid concentration shows positive correlations with all the  
271 other variables. The correlation coefficients between [H<sub>2</sub>SO<sub>4</sub>] and [SO<sub>2</sub>] and between  
272 [H<sub>2</sub>SO<sub>4</sub>] and UVB intensity are 0.74 and 0.46, respectively, consistent with the accepted  
273 formation pathway of gaseous sulfuric acid from the reaction between SO<sub>2</sub> and OH  
274 radicals. Accordingly, [O<sub>3</sub>] and [HONO] show positive correlations with [H<sub>2</sub>SO<sub>4</sub>]  
275 because both O<sub>3</sub> and HONO could be precursors of OH radicals. Surprisingly, a high  
276 positive correlation coefficient (0.6) was found between [H<sub>2</sub>SO<sub>4</sub>] and CS, which is in  
277 contrast to the conventional thought that CS describes the loss of gaseous sulfuric acid  
278 molecules onto pre-existing particles and thus should show a negative correlation. CS  
279 correlates well with [SO<sub>2</sub>] ( $r = 0.83$ ) and [NO<sub>2</sub>] ( $r = 0.77$ ): a high CS value, as an  
280 indicator of an atmospheric particle pollution, is thus usually accompanied with a high  
281 concentration of both SO<sub>2</sub> and NO<sub>2</sub> in urban China, indicating co-emissions. A strong  
282 correlation between [HONO] and [NO<sub>2</sub>] ( $r = 0.88$ ) in our measurement is supported by  
283 the fact that HONO can be heterogeneously formed by reactions of NO<sub>2</sub> on various  
284 surfaces (Calvert et al., 1994).

285 Since the UVB intensity and [SO<sub>2</sub>] have been reported as the dominating factors



286 for the formation of sulfuric acid (Mikkonen et al., 2011; Petäjä et al., 2009), we further  
287 explored the relationship of the measured sulfuric acid concentrations with the UVB  
288 intensity and  $[\text{SO}_2]$  using the nonlinear curve-fitting method with a single variable.  
289 Figure 1a presents a scatter plot of  $[\text{H}_2\text{SO}_4]$  against the UVB intensity, color-coded by  
290  $[\text{SO}_2]$ . A good correlation with a clear lamination by  $[\text{SO}_2]$  is evident, indicating that  
291 the UVB intensity and  $[\text{SO}_2]$  together play an important role in the formation of sulfuric  
292 acid. A similar scatter plot (Figure 1b) of  $[\text{H}_2\text{SO}_4]$  against  $[\text{SO}_2]$ , color-coded by the  
293 UVB intensity, leads to a similar conclusion.

294

### 295 4.3 Proxy construction

296 Similar to the non-linear proxies suggested by Mikkonen et al. (2011), we tested a  
297 number of proxies for gaseous sulfuric acid, listed in Table 3 with their respective fitting  
298 parameters and performance summarized in Table 4. The scatter plots of observed  
299  $[\text{H}_2\text{SO}_4]$  versus predicted values given by proxies are presented in Fig. S1. In these  
300 proxies, the concentration of a gaseous species is in the unit of molecule  $\text{cm}^{-3}$ , the unit  
301 of the UVB intensity is  $\text{W m}^{-2}$ , the unit of CS is  $\text{s}^{-1}$ , and  $k_0$  is a scaling factor.

302 The proxy N1 was built by using the UVB intensity and  $[\text{SO}_2]$  as the source terms  
303 and CS as the sink term, which follows the conventional idea of the  $\text{H}_2\text{SO}_4$  formation  
304 and loss in the atmosphere. CS was then removed from this proxy to examine the  
305 performance of the proxy N2 that have the UVB intensity and  $[\text{SO}_2]$  as the only  
306 predictor variables. Since the formation of OH radicals in the atmosphere depends on  
307 precursors in addition to UVB, we further attempted to introduce the OH precursor term  
308 into the  $\text{H}_2\text{SO}_4$  proxy. The proxies N3 and N4 were built by introducing  $\text{O}_3$  as the only  
309 OH precursor to evaluate its influence on the formation of sulfuric acid. Furthermore,  
310 we added HONO as another potential precursor for OH radicals, resulting in the proxies  
311 N5 and N6. Lastly, the proxy N7 was built by replacing [HONO] with  $[\text{NO}_2]$  because  
312 firstly, HONO is not regularly measured, and secondly, a good linear correlation  
313 between [HONO] and  $[\text{NO}_2]$  was generally observed in the daytime during this  
314 campaign, although higher  $[\text{HONO}]/[\text{NO}_2]$  ratios were observed in the morning due to  
315 the accumulation of HONO during the night (Figure 2). RH was not considered in the  
316 current study because the introduction of RH into the proxy did not yield significantly  
317 better results in the Mikkonen et al. study (2011). In addition to the correlation  
318 coefficient (R), Mean absolute error (MAE) was used to evaluate the performance of  
319 proxies in the statistical analysis.



320 As shown in Table 4, the correlation coefficients are in the range of 0.83-0.86 and  
321 MAEs are in the range of  $(0.94 - 1.03) \times 10^6$  molecule  $\text{cm}^{-3}$ . The exponents for the  
322 UVB intensity range from 0.13 to 0.16, and those for  $[\text{SO}_2]$  generally range from 0.38  
323 to 0.41, except in case of the proxy N6 ( $b=0.33$ ). The obtained exponent  $b$  for  $[\text{SO}_2]$   
324 is significantly smaller than 1 unlike assumed in Eq. (3), mainly because  $[\text{SO}_2]$  is also  
325 an indicator of air pollution that usually influences the sinks of both OH radicals and  
326 sulfuric acid. The exponent for  $[\text{SO}_2]$  ranged from 0.5 to 1.04 in the previous proxy  
327 study for European and North American sites (Mikkonen et al., 2011), including values  
328 from 0.48 to 0.69 in Atlanta, GA, USA, which was probably quite a polluted site  
329 because the measurements were conducted only 9 km away from a coal-fired power  
330 plant. The obtained value range of the exponent  $b$  for  $[\text{SO}_2]$  in our study is probably  
331 related to the urban nature of Beijing. The value of exponent  $c$  for CS in the proxy N1  
332 is as low as 0.03, which either might be due to the covariance of CS and certain  $\text{H}_2\text{SO}_4$   
333 sources that cancels the dependence on CS, or it might indicate that CS is actually  
334 insufficient in regulating the  $\text{H}_2\text{SO}_4$  concentration, as recently suggested by Kulmala et  
335 al. (2017). By comparing the proxies N1 and N2, we can see that CS plays a minor role  
336 because the exponents of  $[\text{SO}_2]$  and UVB, the overall correlation coefficient and the  
337 MAE are almost identical with and without CS. We can see the negligible role of CS  
338 also when comparing the results of the proxies N3 and N4 where  $\text{O}_3$  is considered.  
339 However, the role of CS becomes evident between the proxies N5 and N6 when HONO  
340 is introduced: the exponents of  $[\text{SO}_2]$ ,  $[\text{O}_3]$ , and  $[\text{HONO}]$  significantly increased when  
341 taking into account the CS, suggesting that the covariance between HONO and CS can  
342 explain, at least partially, the close-to-zero exponent of CS in the proxies N1-N4. In  
343 addition, when  $[\text{O}_3]$  is introduced as the only precursor for OH radicals, minor  
344 improvements in the correlation coefficient and MAE were obtained, as suggested by  
345 comparing the proxies N3 and N1. When both  $[\text{O}_3]$  and  $[\text{HONO}]$  were introduced as  
346 OH precursors in the proxies N5-N7, MAE and correlation coefficient significantly  
347 improved. Altogether, these observations suggest that it is crucial to introduce HONO  
348 into the proxy, both in our study and also likely for the previous work where the  
349 exponent of CS is close-to-zero (Mikkonen et al., 2011).

350 Although so far the proxy N5 had the best fitting quality, it is impractical to  
351 explicitly include  $[\text{HONO}]$  because HONO measurements are very challenging. As  
352 shown in Fig. 2,  $[\text{HONO}]$  and  $[\text{NO}_2]$  are tended to correlate linearly with each other in  
353 the daytime during this campaign, with a linearly fitted  $[\text{HONO}]/[\text{NO}_2]$  ratio of around



354 0.03 and a mean absolute error (MAE) of 0.3 ppbv. Similar, strong linearity was  
355 observed in a previous study by Hao et al. (2006) who attributed this observation to the  
356 heterogeneous conversion of NO<sub>2</sub> to HONO. Only occasionally slightly higher  
357 [HONO]/[NO<sub>2</sub>] ratios in the morning could be seen, which might be due to the  
358 deviation from the steady state. Bernard et al. (2016) reported that [NO<sub>2</sub>] has a similar  
359 diurnal behavior to that of [HONO] and hence the ratio of [HONO]/[NO<sub>2</sub>] varies  
360 slightly during the diurnal cycle. Therefore, due to the good correlation, the proxy N7  
361 replaces [HONO] by [NO<sub>2</sub>], a more easily measured variable, and performs equally  
362 well with the proxy N5.

363 Clearly, the proxy N2 provides the simplest parameterization, but the proxies N5  
364 and N7 result in the best fitting quality because of the introduction of [HONO]. Figure  
365 3a and 3b present the averaged and relative deviation of calculated sulfuric acid  
366 concentrations according to the proxies N2 and N7, respectively, as a function of linear  
367 bins of measured sulfuric acid concentrations. The averaged and relative deviation are  
368 defined by Eq. (6) and Eq. (7), respectively, assuming that there are a number of  $j$  data  
369 points, both measured and calculated, in the  $i^{\text{th}}$  bin.

370

$$371 \quad \textit{Averaged deviation} = \frac{1}{n} \cdot \sum_{j=1}^n ([H_2SO_4]_{\text{proxy},ij} - [H_2SO_4]_{\text{meas},ij}) \quad (6)$$

$$372 \quad \textit{Relative deviation} = \frac{1}{n} \cdot \sum_{j=1}^n \frac{([H_2SO_4]_{\text{proxy},ij} - [H_2SO_4]_{\text{meas},ij})}{[H_2SO_4]_{\text{meas},ij}} \quad (7)$$

373

374 The performance of the proxy N7 is considerably better than that of the proxy N2  
375 in the sulfuric acid concentration range of  $(2.0 - 15) \times 10^6$  molecule cm<sup>-3</sup>, which  
376 covers most measured concentrations of sulfuric acid. The relative deviation is less than  
377 24% for all the bins in case of the proxy N7, rising up to 29% in case of the proxy N2.  
378 For the first bin in a range of  $(1.0 - 2.0) \times 10^6$  molecules cm<sup>-3</sup>, both proxy N2 and  
379 N7 show small averaged deviations but the biggest relative deviations, which is due to  
380 the smallest denominators. Since we want to make it clear in which bins the predicted  
381 values are overestimated or underestimated in Fig. 3a and 3b, the calculation method  
382 from Eq. (6) and Eq. (7) would make the positive derivations and negative derivations  
383 counteracted to some extent, which is obvious in the middle bins.

384



#### 385 4.4 Comparison of measured and predicted [H<sub>2</sub>SO<sub>4</sub>]

386 A comparison between measured and predicted [H<sub>2</sub>SO<sub>4</sub>] was performed. Figure 4  
387 includes calculated results from the proxies N2 and N7 as well as from a proxy  
388 constructed according to measurement in a boreal forest site, Finland, *i.e.*, Eq (1) (Petäjä  
389 *et al.*, 2009). The measured daytime [H<sub>2</sub>SO<sub>4</sub>] on 10 March, 2018, was above  $4 \times 10^6$   
390 molecules cm<sup>-3</sup> with a time resolution of 5 min. The predicted [H<sub>2</sub>SO<sub>4</sub>] using the proxies  
391 N2 and N7 both track the measured [H<sub>2</sub>SO<sub>4</sub>] pretty well, even when an unexpected dip  
392 in the sulfuric acid concentration was observed at around 10:00-11:00. The  
393 performance of the proxy N7 is better than that of proxy N2 during the entire day,  
394 consistent with our results in Fig. 3. The proxy by Petäjä *et al.* (2009) underestimated  
395 the concentrations of sulfuric acid by a factor of 20 or so, which can be attributed to the  
396 very different values of CS between Beijing and the boreal forest. The fact that  
397 [H<sub>2</sub>SO<sub>4</sub>]<sub>Petäjä *et al.*</sub> does not track the measured [H<sub>2</sub>SO<sub>4</sub>] even after including a scaling  
398 factor indicates that proxies are site-specific and do not necessarily work well in  
399 locations other than where they have originally been developed for. In addition, the  
400 direct performance comparison between the proxy N2 and the proxy by Petäjä *et al.*  
401 (2009) indicates the importance of assigning exponential weights to variables in the  
402 nonlinear fitting procedures, which is consistent with results by Mikkonen *et al.* (2011).

403

#### 404 5 Summary and conclusions

405 Sulfuric acid is a key precursor for atmospheric new particle formation. In this  
406 study, we constructed a number of proxies for gaseous sulfuric acid concentration  
407 according to our measurements in urban Beijing during the winter. According to the  
408 obtained proxies and their performance, the UVB intensity and [SO<sub>2</sub>] were the  
409 dominant influencing factors. Hence, the simplest proxy (Proxy N2) only involves  
410 UVB intensity and [SO<sub>2</sub>] as shown by Eq. (8).

412

$$411 \quad [H_2SO_4] = 280.05 \cdot UVB^{0.14} \cdot [SO_2]^{0.40} \quad (8)$$

413

414 This proxy resulted in a relative deviation of up to 29 %.

415 For the best proxy accuracy, [O<sub>3</sub>] and [HONO] as well as CS should be included  
416 (Proxy N5), as shown by Eq. (9):

417



$$[H_2SO_4] = 0.0072 \cdot UVB^{0.15} \cdot [SO_2]^{0.41} \cdot CS^{-0.17} \cdot ([O_3]^{0.36} + [HONO]^{0.38}) \quad (9)$$

Since HONO measurements are not a regular practice, we can further replace [HONO] with [NO<sub>2</sub>], shown in Eq. (10), which can be justified by the strong linear correlation between [HONO] and [NO<sub>2</sub>] observed in this study:

$$[H_2SO_4] = 0.0013 \cdot UVB^{0.13} \cdot [SO_2]^{0.40} \cdot CS^{-0.17} \cdot ([O_3]^{0.44} + [NO_2]^{0.41}) \quad (10)$$

We consider this last proxy more reasonable than the others due to the following reasons: first, it makes the equation physically meaningful as the CS starts to be involved as a sink term, and second, the absolute and relative fitting error were reduced considerably compared with the other proxies. Overall, this suggests that the photolysis of O<sub>3</sub> and HONO are both important OH sources in urban Beijing.

As a summary, we recommend using the simplest proxy (proxy N2) and a more accurate proxy (Proxy N7) for calculating daytime gaseous sulfuric acid concentrations in the urban Beijing atmosphere. It is clear that the current proxies are based on only a month-long campaign of sulfuric acid measurements in urban Beijing during winter. Given the dramatic reduction in the concentration of SO<sub>2</sub> in recent years (Wang et al., 2018) and the strong dependence of calculated [H<sub>2</sub>SO<sub>4</sub>] on [SO<sub>2</sub>], the performance of the proxies in the past and future years remain to be evaluated. Nevertheless, our work here shows the importance of heterogeneous chemistry as a potential source of OH radicals in an urban air; however, the proxies might be site-specific and should be further tested before their application to other Chinese megacities.

#### Author contributions

LW designed this study. YL (Yiqun Lu), CY, YF, YC, YL (Yiliang Liu), GY, YW, YZ, RY, RB and CD conducted the field campaign. YL (Yiqun Lu) analyzed data with contributions from LW and all the other co-authors. YL (Yiqun Lu) and LW wrote the manuscript with contributions from all the other co-authors.

#### Acknowledgement

This study was financially supported by the National Key R&D Program of China



452 (2017YFC0209505), and the National Natural Science Foundation of China (41575113,  
453 91644213).

454 **References**

- 455 Acker, K., Möller, D., Auel, R., Wieprecht, W. and Kalaß, D.: Concentrations of nitrous acid, nitric  
456 acid, nitrite and nitrate in the gas and aerosol phase at a site in the emission zone during  
457 ESCOMPTE 2001 experiment, *Atmos. Res.*, 74(1–4), 507–524,  
458 doi:10.1016/j.atmosres.2004.04.009, 2005.
- 459 Alicke, B., Platt, U. and Stutz, J.: Impact of nitrous acid photolysis on the total hydroxyl radical  
460 budget during the Limitation of Oxidant Production/Pianura Padana Produzione di Ozono  
461 study in Milan, *J. Geophys. Res. Atmos.*, 107(22), doi:10.1029/2000JD000075, 2002.
- 462 Alicke, B., Geyer, A., Hofzumahaus, A., Holland, F., Konrad, S., Patz, H. W., Schafer, J., Stutz, J.,  
463 Volz-Thomas, A. and Platt, U.: OH formation by HONO photolysis during the BERLIOZ  
464 experiment, *J. Geophys. Res.*, 108(D4), 8247, doi:10.1029/2001JD000579, 2003.
- 465 Almeida, J., Schobesberger, S., Kürten, A., Ortega, I. K., Kupiainen-Määttä, O., Praplan, A. P.,  
466 Adamov, A., Amorim, A., Bianchi, F., Breitenlechner, M., David, A., Dommen, J., Donahue,  
467 N. M., Downard, A., Dunne, E., Duplissy, J., Ehrhart, S., Flagan, R. C., Franchin, A., Guida,  
468 R., Hakala, J., Hansel, A., Heinritzi, M., Henschel, H., Jokinen, T., Junninen, H., Kajos, M.,  
469 Kangasluoma, J., Keskinen, H., Kupc, A., Kurtén, T., Kvashin, A. N., Laaksonen, A., Lehtipalo,  
470 K., Leiminger, M., Leppä, J., Loukonen, V., Makhmutov, V., Mathot, S., McGrath, M. J.,  
471 Nieminen, T., Olenius, T., Onnela, A., Petäjä, T., Riccobono, F., Riipinen, I., Rissanen, M.,  
472 Rondo, L., Ruuskanen, T., Santos, F. D., Sarnela, N., Schallhart, S., Schnitzhofer, R., Seinfeld,  
473 J. H., Simon, M., Sipilä, M., Stozhkov, Y., Stratmann, F., Tomé, A., Tröstl, J., Tsagkogeorgas,  
474 G., Vaattovaara, P., Viisanen, Y., Virtanen, A., Vrtala, A., Wagner, P. E., Weingartner, E.,  
475 Wex, H., Williamson, C., Wimmer, D., Ye, P., Yli-Juuti, T., Carslaw, K. S., Kulmala, M.,  
476 Curtius, J., Baltensperger, U., Worsnop, D. R., Vehkamäki, H. and Kirkby, J.: Molecular  
477 understanding of sulphuric acid-amine particle nucleation in the atmosphere, *Nature*,  
478 502(7471), 359–363, doi:10.1038/nature12663, 2013.
- 479 Arnold, F. and Fabian, R.: First measurements of gas phase sulphuric acid in the stratosphere, *Nature*,  
480 283(3), 55–57, 1980.
- 481 Aumont, B., Chervier, F. and Laval, S.: Contribution of HONO sources to the NO<sub>x</sub>/HO<sub>x</sub>/O<sub>3</sub>  
482 chemistry in the polluted boundary layer, *Atmos. Environ.*, 37(4), 487–498,  
483 doi:10.1016/S1352-2310(02)00920-2, 2003.
- 484 Benson, D. R., Young, L. H., Kameel, F. R. and Lee, S. H.: Laboratory-measured nucleation rates  
485 of sulfuric acid and water binary homogeneous nucleation from the SO<sub>2</sub> + OH reaction,  
486 *Geophys. Res. Lett.*, 35(11), 1–6, doi:10.1029/2008GL033387, 2008.
- 487 Bernard, F., Cazaunau, M., Grosselein, B., Zhou, B., Zheng, J., Liang, P., Zhang, Y., Ye, X., Daële,  
488 V., Mu, Y., Zhang, R., Chen, J. and Mellouki, A.: Measurements of nitrous acid (HONO) in  
489 urban area of Shanghai, China, *Environ. Sci. Pollut. Res.*, 23(6), 5818–5829,  
490 doi:10.1007/s11356-015-5797-4, 2016.
- 491 Berresheim, H., Elste, T., Plass-Dülmer, C., Eisele, F. L. and Tanner, D. J.: Chemical ionization  
492 mass spectrometer for long-term measurements of atmospheric OH and H<sub>2</sub>SO<sub>4</sub>, *Int. J. Mass  
493 Spectrom.*, 202(1–3), 91–109, doi:10.1016/S1387-3806(00)00233-5, 2000.
- 494 Bianchi, F., Tröstl, J., Junninen, H., Frege, C., Henne, S., Hoyle, C. R., Molteni, U., Herrmann, E.,  
495 Adamov, A., Bukowiecki, N., Chen, X., Duplissy, J., Gysel, M., Hutterli, M., Kangasluoma,





- 496 J., Kontkanen, J., Kurten, A., Manninen, H. E., Munch, S., Peräkylä, O., Petäjä, T., Rondo, L.,  
497 Williamson, C., Weingartner, E., Curtius, J., Worsnop, D. R., Kulmala, M., Dommen, J. and  
498 Baltensperger, U.: New particle formation in the free troposphere: A question of chemistry and  
499 timing, *Science*, 352(6289), 1109–1112, doi:10.1126/science.aad5456, 2016.
- 500 Boy, M., Mogensen, D., Smolander, S., Zhou, L., Nieminen, T., Paasonen, P., Plass-Dülmer, C.,  
501 Sipilä, M., Petäjä, T., Mauldin, L., Berresheim, H. and Kulmala, M.: Oxidation of SO<sub>2</sub> by  
502 stabilized Criegee intermediate (sCI) radicals as a crucial source for atmospheric sulfuric acid  
503 concentrations, *Atmos. Chem. Phys.*, 13(7), 3865–3879, doi:10.5194/acp-13-3865-2013, 2013.
- 504 Cai, R., Chen, D. R., Hao, J. and Jiang, J.: A miniature cylindrical differential mobility analyzer for  
505 sub-3 nm particle sizing, *J. Aerosol Sci.*, 106(September 2016), 111–119,  
506 doi:10.1016/j.jaerosci.2017.01.004, 2017.
- 507 Calvert, J. G., Yarwood, G. and Dunker, A. M.: An evaluation of the mechanism of nitrous acid  
508 formation in the urban atmosphere, *Res. Chem. Intermed.*, 20(3–5), 463–502,  
509 doi:10.1163/156856794X00423, 1994.
- 510 Crutzen, P. J. and Zimmermann, P. H.: The changing photochemistry of the troposphere, *Tellus*,  
511 43AB(December), 136–151, doi:10.3402/tellusb.v43i4.15397, 1991.
- 512 Dal Maso, M., Kulmala, M., Lehtinen, K. E. J., Mkelä, J. M., Aalto, P. and O’Dowd, C. D.:  
513 Condensation and coagulation sinks and formation of nucleation mode particles in coastal and  
514 boreal forest boundary layers, *J. Geophys. Res. Atmos.*, 107(19), doi:10.1029/2001JD001053,  
515 2002.
- 516 DeMore, W. B., Sander, S. P., Golden, D. M., Hampson, R. F., Kurylo, M. J., Howard, C. J.,  
517 Ravishankara, A. R., Kolb, C. E. and Molina, M. J.: Chemical kinetics and photochemical data  
518 for use in stratospheric modeling, *JPL Publ.*, 97–4(12), 278, doi:10.1002/kin.550171010, 1997.
- 519 Duplissy, J., Merikanto, J., Franchin, A., Tsagkogeorgas, G., Kangasluoma, J., Wimmer, D.,  
520 Vuollekoski, H., Schobesberger, S., Lehtipalo, K., Flagan, R. C., Brus, D., Donahue, N. M.,  
521 Vehkamäki, H., Almeida, J., Amorim, A., Barmet, P., Bianchi, F., Breitenlechner, M., Dunne,  
522 E. M., Guida, R., Henschel, H., Junninen, H., Kirkby, J., Kürten, A., Kupc, A., Määttänen, A.,  
523 Makhmutov, V., Mathot, S., Nieminen, T., Onnela, A., Praplan, A. P., Riccobono, F., Rondo,  
524 L., Steiner, G., Tome, A., Walther, H., Baltensperger, U., Carslaw, K. S., Dommen, J., Hansel,  
525 A., Petäjä, T., Sipilä, M., Stratmann, F., Vrtala, A., Wagner, P. E., Worsnop, D. R., Curtius, J.  
526 and Kulmala, M.: Effect of dimethylamine on the gas phase sulfuric acid concentration  
527 measured by Chemical Ionization Mass Spectrometry, *J. Geophys. Res. Atmos.*, 1752–1775,  
528 doi:10.1002/2015JD023538.Effect, 2016.
- 529 Eisele, F. L. and Tanner, D. J.: Measurement of the gas phase concentration of H<sub>2</sub>SO<sub>4</sub> and methane  
530 sulfonic acid and estimates of H<sub>2</sub>SO<sub>4</sub> production and loss in the atmosphere, *J. Geophys. Res.*  
531 *Atmos.*, 98(D5), 9001–9010, doi:10.1029/93JD00031, 1993.
- 532 Elshorbany, Y. F., Kurtenbach, R., Wiesen, P., Lissi, E., Rubio, M., Villena, G., Gramsch, E.,  
533 Rickard, A. R., Pilling, M. J. and Kleffmann, J.: Oxidation capacity of the city air of Santiago,  
534 Chile, *Atmos. Chem. Phys.*, doi:10.5194/acp-9-2257-2009, 2009.
- 535 Finlayson-Pitts, B. J. and Pitts, J. N.: Acid Deposition: Formation and Fates of Inorganic and  
536 Organic Acids in the Troposphere, in *Chemistry of the Upper and Lower Atmosphere: Theory,*  
537 *Experiments, and Applications*, p. 969, Academic Press, San Diego., 2000.



- 538 Fuchs, N. A. and Sutugin, A. G.: Highly dispersed aerosols, in Topics in Current Aerosol Research,  
539 edited by G. M. HIDY and J. R. BROCK, p. 1, Pergamon., 1971.
- 540 Hao, N., Zhou, B., Chen, D. and Chen, L. min: Observations of nitrous acid and its relative humidity  
541 dependence in Shanghai, *J. Environ. Sci. (China)*, 18(5), 910–915, doi:10.1016/S1001-  
542 0742(06)60013-2, 2006.
- 543 Hendrick, F., Clémer, K., Wang, P., De Mazière, M., Fayt, C., Gielen, C., Hermans, C., Ma, J. Z.,  
544 Pinardi, G., Stavrakou, T., Vlemmix, T. and Van Roozendaal, M.: Four years of ground-based  
545 MAX-DOAS observations of HONO and NO<sub>2</sub> in the Beijing area, *Atmos. Chem. Phys.*, 14(2),  
546 765–781, doi:10.5194/acp-14-765-2014, 2014.
- 547 Herrmann, E., Ding, A. J., Kerminen, V. M., Petäjä, T., Yang, X. Q., Sun, J. N., Qi, X. M., Manninen,  
548 H., Hakala, J., Nieminen, T., Aalto, P. P., Kulmala, M. and Fu, C. B.: Aerosols and nucleation  
549 in eastern China: First insights from the new SORPES-NJU station, *Atmos. Chem. Phys.*, 14(4),  
550 2169–2183, doi:10.5194/acp-14-2169-2014, 2014.
- 551 Jiang, J., Zhao, J., Chen, M., Eisele, F. L., Scheckman, J., Williams, B. J., Kuang, C. and McMurry,  
552 P. H.: First measurements of neutral atmospheric cluster and 1-2 nm particle number size  
553 distributions during nucleation events, *Aerosol Sci. Technol.*, 45(4),  
554 doi:10.1080/02786826.2010.546817, 2011.
- 555 Jokinen, T., Sipilä, M., Junninen, H., Ehn, M., Lönn, G., Hakala, J., Petäjä, T., Mauldin, R. L.,  
556 Kulmala, M. and Worsnop, D. R.: Atmospheric sulphuric acid and neutral cluster  
557 measurements using CI-API-TOF, *Atmos. Chem. Phys.*, 12(9), 4117–4125, doi:10.5194/acp-  
558 12-4117-2012, 2012.
- 559 Junninen, H., Ehn, M., Petäjä, Luosujärvi, L., Kotiaho, T., Kostianinen, R., Rohner, U., Gonin, M.,  
560 Fuhrer, K., Kulmala, M. and Worsnop, D. R.: A high-resolution mass spectrometer to measure  
561 atmospheric ion composition, *Atmos. Meas. Tech.*, 3(4), 1039–1053, doi:10.5194/amt-3-1039-  
562 2010, 2010.
- 563 Kerminen, V.: Atmospheric new particle formation and growth: review of field observations,  
564 *Environ. Res. Lett.*, 13, 103003, 2018.
- 565 Kerminen, V. M., Petäjä, T., Manninen, H. E., Paasonen, P., Nieminen, T., Sipilä, M., Junninen, H.,  
566 Ehn, M., Gagné, S., Laakso, L., Riipinen, I., Vehkämäki, H., Kurtén, T., Ortega, I. K., Dal  
567 Maso, M., Brus, D., Hyvärinen, A., Lihavainen, H., Leppä, J., Lehtinen, K. E. J., Mirme, A.,  
568 Mirme, S., Hörrak, U., Berndt, T., Stratmann, F., Birmili, W., Wiedensohler, A., Metzger, A.,  
569 Dommen, J., Baltensperger, U., Kiendler-Scharr, A., Mentel, T. F., Wildt, J., Winkler, P. M.,  
570 Wagner, P. E., Petzold, A., Minikin, A., Plass-Dülmer, C., Pöschl, U., Laaksonen, A. and  
571 Kulmala, M.: Atmospheric nucleation: Highlights of the EUCAARI project and future  
572 directions, *Atmos. Chem. Phys.*, 10(22), 10829–10848, doi:10.5194/acp-10-10829-2010, 2010.
- 573 Kirkby, J., Curtius, J., Almeida, J., Dunne, E., Duplissy, J., Ehrhart, S., Franchin, A., Gagné, S.,  
574 Ickes, L., Kürten, A., Kupc, A., Metzger, A., Riccobono, F., Rondo, L., Schobesberger, S.,  
575 Tsagkogeorgas, G., Wimmer, D., Amorim, A., Bianchi, F., Breitenlechner, M., David, A.,  
576 Dommen, J., Downard, A., Ehn, M., Flagan, R. C., Haider, S., Hansel, A., Hauser, D., Jud, W.,  
577 Junninen, H., Kreissl, F., Kvashin, A., Laaksonen, A., Lehtipalo, K., Lima, J., Lovejoy, E. R.,  
578 Makhmutov, V., Mathot, S., Mikkilä, J., Minginette, P., Mogo, S., Nieminen, T., Onnela, A.,  
579 Pereira, P., Petäjä, T., Schnitzhofer, R., Seinfeld, J. H., Sipilä, M., Stozhkov, Y., Stratmann, F.,



- 580 Tomé, A., Vanhanen, J., Viisanen, Y., Vrtala, A., Wagner, P. E., Walther, H., Weingartner, E.,  
581 Wex, H., Winkler, P. M., Carslaw, K. S., Worsnop, D. R., Baltensperger, U. and Kulmala, M.:  
582 Role of sulphuric acid, ammonia and galactic cosmic rays in atmospheric aerosol nucleation,  
583 *Nature*, 476, 429 [online] Available from: <http://dx.doi.org/10.1038/nature10343>, 2011.
- 584 Kleffmann, J.: Daytime sources of nitrous acid (HONO) in the atmospheric boundary layer,  
585 *ChemPhysChem*, 8(8), 1137–1144, doi:10.1002/cphc.200700016, 2007.
- 586 Korhonen, P., Kulmala, M., Laaksonen, A., Viisanen, Y., McGraw, R. and Seinfeld, J. H.: Ternary  
587 nucleation of H<sub>2</sub>SO<sub>4</sub>, NH<sub>3</sub>, and H<sub>2</sub>O in the atmosphere, *J. Geophys. Res.*,  
588 doi:10.1029/1999JD900784, 1999.
- 589 Kuang, C., McMurry, P. H., McCormick, A. V. and Eisele, F. L.: Dependence of nucleation rates  
590 on sulfuric acid vapor concentration in diverse atmospheric locations, *J. Geophys. Res. Atmos.*,  
591 113(10), 1–9, doi:10.1029/2007JD009253, 2008.
- 592 Kulmala, M. and Kerminen, V. M.: On the formation and growth of atmospheric nanoparticles,  
593 *Atmos. Res.*, 90(2–4), 132–150, doi:10.1016/j.atmosres.2008.01.005, 2008.
- 594 Kulmala, M., Petäjä, T., Nieminen, T., Sipilä, M., Manninen, H. E., Lehtipalo, K., Dal Maso, M.,  
595 Aalto, P. P., Junninen, H., Paasonen, P., Riipinen, I., Lehtinen, K. E. J., Laaksonen, A. and  
596 Kerminen, V.-M.: Measurement of the nucleation of atmospheric aerosol particles, *Nat. Protoc.*,  
597 7(9), 1651–1667, doi:10.1038/nprot.2012.091, 2012.
- 598 Kulmala, M., Kontkanen, J., Junninen, H., Lehtipalo, K., Manninen, H. E., Nieminen, T., Petäjä, T.,  
599 Sipilä, M., Schobesberger, S., Rantala, P., Franchin, A., Jokinen, T., Järvinen, E., Äijälä, M.,  
600 Kangasluoma, J., Hakala, J., Aalto, P. P., Paasonen, P., Mikkilä, J., Vanhanen, J., Aalto, J.,  
601 Hakola, H., Makkonen, U., Ruuskanen, T., Mauldin, R. L., Duplissy, J., Vehkamäki, H., Bäck,  
602 J., Kortelainen, A., Riipinen, I., Kurtén, T., Johnston, M. V., Smith, J. N., Ehn, M., Mentel, T.  
603 F., Lehtinen, K. E. J., Laaksonen, A., Kerminen, V. M. and Worsnop, D. R.: Direct  
604 observations of atmospheric aerosol nucleation, *Science*, 339(6122), 943–946,  
605 doi:10.1126/science.1227385, 2013.
- 606 Kulmala, M., Kerminen, V.-M., Petäjä, T., Ding, A. J. and Wang, L.: Atmospheric gas-to-particle  
607 conversion: why NPF events are observed in megacities?, *Faraday Discuss.*, 200(0), 271–288,  
608 doi:10.1039/C6FD00257A, 2017.
- 609 Kürten, A., Rondo, L., Ehrhart, S. and Curtius, J.: Calibration of a chemical ionization mass  
610 spectrometer for the measurement of gaseous sulfuric acid, *J. Phys. Chem. A*, 116(24), 6375–  
611 6386, doi:10.1021/jp212123n, 2012.
- 612 Kürten, A., Jokinen, T., Simon, M., Sipilä, M., Sarnela, N., Junninen, H., Adamov, A., Almeida, J.,  
613 Amorim, A., Bianchi, F., Breitenlechner, M., Dommen, J., Donahue, N. M., Duplissy, J.,  
614 Ehrhart, S., Flagan, R. C., Franchin, A., Hakala, J., Hansel, A., Heinritzi, M., Hutterli, M.,  
615 Kangasluoma, J., Kirkby, J., Laaksonen, A., Lehtipalo, K., Leiminger, M., Makhmutov, V.,  
616 Mathot, S., Onnela, A., Petäjä, T., Praplan, A. P., Riccobono, F., Rissanen, M. P., Rondo, L.,  
617 Schobesberger, S., Seinfeld, J. H., Steiner, G., Tomé, A., Tröstl, J., Winkler, P. M., Williamson,  
618 C., Wimmer, D., Ye, P., Baltensperger, U., Carslaw, K. S., Kulmala, M., Worsnop, D. R. and  
619 Curtius, J.: Neutral molecular cluster formation of sulfuric acid-dimethylamine observed in  
620 real time under atmospheric conditions, *Proc. Natl. Acad. Sci.*, 111(42), 15019–15024,  
621 doi:10.1073/pnas.1404853111, 2014.



- 622 Kürten, A., Münch, S., Rondo, L., Bianchi, F., Duplissy, J., Jokinen, T., Junninen, H., Sarnela, N.,  
623 Schobesberger, S., Simon, M., Sipilä, M., Almeida, J., Amorim, A., Dommen, J., Donahue, N.  
624 M., Dunne, E. M., Flagan, R. C., Franchin, A., Kirkby, J., Kupc, A., Makhmutov, V., Petäjä,  
625 T., Praplan, A. P., Riccobono, F., Steiner, G., Tomé, A., Tsagkogeorgas, G., Wagner, P. E.,  
626 Wimmer, D., Baltensperger, U., Kulmala, M., Worsnop, D. R. and Curtius, J.:  
627 Thermodynamics of the formation of sulfuric acid dimers in the binary (H<sub>2</sub>SO<sub>4</sub>-H<sub>2</sub>O) and  
628 ternary (H<sub>2</sub>SO<sub>4</sub>-H<sub>2</sub>O-NH<sub>3</sub>) system, *Atmos. Chem. Phys.*, 15(18), 10701–10721,  
629 doi:10.5194/acp-15-10701-2015, 2015.
- 630 Kurtén, T., Petäjä, T., Smith, J., Ortega, I. K., Sipilä, M., Junninen, H., Ehn, M., Vehkamäki, H.,  
631 Mauldin, L., Worsnop, D. R. and Kulmala, M.: The effect of H<sub>2</sub>SO<sub>4</sub>-amine clustering on  
632 chemical ionization mass spectrometry (CIMS) measurements of gas-phase sulfuric acid,  
633 *Atmos. Chem. Phys.*, 11(6), 3007–3019, doi:10.5194/acp-11-3007-2011, 2011.
- 634 Li, X., Brauers, T., Häsel, R., Bohn, B., Fuchs, H., Hofzumahaus, A., Holland, F., Lou, S., Lu, K.,  
635 D., Rohrer, F., Hu, M., Zeng, L. M., Zhang, Y. H., Garland, R. M., Su, H., Nowak, A.,  
636 Wiedensohler, A., Takegawa, N., Shao, M. and Wahner, A.: Exploring the atmospheric  
637 chemistry of nitrous acid (HONO) at a rural site in Southern China, *Atmos. Chem. Phys.*, 12(3),  
638 1497–1513, doi:10.5194/acp-12-1497-2012, 2012.
- 639 Liu, J., Jiang, J., Zhang, Q., Deng, J. and Hao, J.: A spectrometer for measuring particle size  
640 distributions in the range of 3 nm to 10 μm, *Front. Environ. Sci. Eng.*, 10(1), 63–72,  
641 doi:10.1007/s11783-014-0754-x, 2016.
- 642 Logan, J. A., Prather, M. J., Wofsy, S. C. and McElroy, M. B.: Tropospheric chemistry: A global  
643 perspective, *J. Geophys. Res.*, 86(C8), 7210–7254, doi:10.1029/JC086iC08p07210, 1981.
- 644 Mauldin, R. L., Berndt, T., Sipilä, M., Paasonen, P., Petäjä, T., Kim, S., Kurtén, T., Stratmann, F.,  
645 Kerminen, V. M. and Kulmala, M.: A new atmospherically relevant oxidant of sulphur dioxide,  
646 *Nature*, 488(7410), 193–196, doi:10.1038/nature11278, 2012.
- 647 Mikkonen, S., Romakkaniemi, S., Smith, J. N., Korhonen, H., Petäjä, T., Plass-Dümler, C., Boy,  
648 M., McMurry, P. H., Lehtinen, K. E. J., Joutsensaari, J., Hamed, A., Mauldin, R. L., Birmili,  
649 W., Spindler, G., Arnold, F., Kulmala, M. and Laaksonen, A.: A statistical proxy for sulphuric  
650 acid concentration, *Atmos. Chem. Phys.*, 11(21), 11319–11334, doi:10.5194/acp-11-11319-  
651 2011, 2011.
- 652 Nieminen, T., Lehtinen, K. E. J. and Kulmala, M.: Sub-10 nm particle growth by vapor  
653 condensation-effects of vapor molecule size and particle thermal speed, *Atmos. Chem. Phys.*,  
654 10(20), 9773–9779, doi:10.5194/acp-10-9773-2010, 2010.
- 655 Paasonen, P., Nieminen, T., Asmi, E., Manninen, H. E., Petäjä, T., Plass-Dümler, C., Flentje, H.,  
656 Birmili, W., Wiedensohler, A., Hörrak, U., Metzger, A., Hamed, A., Laaksonen, A., Facchini,  
657 M. C., Kerminen, V. M. and Kulmala, M.: On the roles of sulphuric acid and low-volatility  
658 organic vapours in the initial steps of atmospheric new particle formation, *Atmos. Chem. Phys.*,  
659 10(22), 11223–11242, doi:10.5194/acp-10-11223-2010, 2010.
- 660 Petäjä, T., Mauldin, R. L., Kosciuch, E., McGrath, J., Nieminen, T., Paasonen, P., Boy, M., Adamov,  
661 A., Kotiaho, T. and Kulmala, M.: Sulfuric acid and OH concentrations in a boreal forest site,  
662 *Atmos. Chem. Phys.*, 9(19), 7435–7448, doi:10.5194/acp-9-7435-2009, 2009.
- 663 Petäjä, T., Sipilä, M., Paasonen, P., Nieminen, T., Kurtén, T., Ortega, I. K., Stratmann, F.,



- 664 Vekkamäki, H., Berndt, T. and Kulmala, M.: Experimental observation of strongly bound  
665 dimers of sulfuric acid: Application to nucleation in the atmosphere, *Phys. Rev. Lett.*, 106(22),  
666 1–4, doi:10.1103/PhysRevLett.106.228302, 2011.
- 667 Pirjola, L., Kulmala, M., Wilck, M., Bischoff, A., Stratmann, F. and Otto, E.: Formation of sulphuric  
668 acid aerosols and cloud condensation nuclei: An expression for significant nucleation and  
669 model comparison, *J. Aerosol Sci.*, doi:10.1016/S0021-8502(98)00776-9, 1999.
- 670 Rohrer, F. and Berresheim, H.: Strong correlation between levels of tropospheric hydroxyl radicals  
671 and solar ultraviolet radiation, *Nature*, 442(7099), 184–187, doi:10.1038/nature04924, 2006.
- 672 Sipilä, M., Berndt, T., Petäjä, T., Brus, D., Vanhanen, J., Stratmann, F., Patokoski, J., Mauldin, R.  
673 L., Hyvärinen, A. P., Lihavainen, H. and Kulmala, M.: The role of sulfuric acid in atmospheric  
674 nucleation, *Science*, 327(5970), 1243–1246, doi:10.1126/science.1180315, 2010.
- 675 Spataro, F., Ianniello, A., Esposito, G., Allegrini, I., Zhu, T. and Hu, M.: Occurrence of atmospheric  
676 nitrous acid in the urban area of Beijing (China), *Sci. Total Environ.*, 447, 210–224,  
677 doi:10.1016/j.scitotenv.2012.12.065, 2013.
- 678 Stockwell, W. R. and Calvert, J. G.: The mechanism of the HO-SO<sub>2</sub> reaction, *Atmos. Environ.*,  
679 17(11), 2231–2235, doi:10.1016/0004-6981(83)90220-2, 1983.
- 680 Su, H., Cheng, Y., Oswald, R., Behrendt, T., Trebs, I., Meixner, F. X., Andreae, M. O., Cheng, P.,  
681 Zhang, Y. and Pöschl, U.: Soil nitrite as a source of atmospheric HONO and OH radicals,  
682 *Science*, 333(6049), 1616–1618, doi:10.1126/science.1207687, 2011.
- 683 Tong, S., Hou, S., Zhang, Y., Chu, B., Liu, Y., He, H., Zhao, P. and Ge, M.: Exploring the nitrous  
684 acid (HONO) formation mechanism in winter Beijing: Direct emissions and heterogeneous  
685 production in urban and suburban areas, *Faraday Discuss.*, 189, 213–230,  
686 doi:10.1039/c5fd00163c, 2016.
- 687 Villena, G., Wiesen, P., Cantrell, C. A., Flocke, F., Fried, A., Hall, S. R., Hornbrook, R. S., Knapp,  
688 D., Kosciuch, E., Mauldin, R. L., McGrath, J. A., Montzka, D., Richter, D., Ullmann, K.,  
689 Walega, J., Weibring, P., Weinheimer, A., Staebler, R. M., Liao, J., Huey, L. G. and Kleffmann,  
690 J.: Nitrous acid (HONO) during polar spring in Barrow, Alaska: A net source of OH radicals?,  
691 *J. Geophys. Res. Atmos.*, 116(24), 1–12, doi:10.1029/2011JD016643, 2011.
- 692 Wang, J., Zhang, X., Guo, J., Wang, Z. and Zhang, M.: Observation of nitrous acid (HONO) in  
693 Beijing, China: Seasonal variation, nocturnal formation and daytime budget, *Sci. Total  
694 Environ.*, 587–588, 350–359, doi:10.1016/j.scitotenv.2017.02.159, 2017.
- 695 Wang, M., Zhu, T., Zhang, J. P., Zhang, Q. H., Lin, W. W., Li, Y. and Wang, Z. F.: Using a mobile  
696 laboratory to characterize the distribution and transport of sulfur dioxide in and around Beijing,  
697 *Atmos. Chem. Phys.*, 11(22), 11631–11645, doi:10.5194/acp-11-11631-2011, 2011a.
- 698 Wang, Z., Zheng, F., Zhang, W. and Wang, S.: Analysis of SO<sub>2</sub> Pollution Changes of Beijing-  
699 Tianjin-Hebei Region over China Based on OMI Observations from 2006 to 2017, *Adv.  
700 Meteorol.*, 2018, Article ID 8746068, 2018.
- 701 Wang, Z. B., Hu, M., Yue, D. L., Zheng, J., Zhang, R. Y., Wiedensohler, A., Wu, Z. J., Nieminen,  
702 T. and Boy, M.: Evaluation on the role of sulfuric acid in the mechanisms of new particle  
703 formation for Beijing case, *Atmos. Chem. Phys.*, 11(24), 12663–12671, doi:10.5194/acp-11-  
704 12663-2011, 2011b.
- 705 Weber, R. J., Marti, J. J., McMurry, P. H., Eisele, F. L., Tanner, D. J. and Jefferson, a.:



- 706 Measurements of new particle formation and ultrafine particle growth rates at a clean  
707 continental site, *J. Geophys. Res. Atmos.*, 102, 4375–4385, doi:10.1029/96JD03656, 1997.
- 708 Wu, F., Xie, P., Li, A., Mou, F., Chen, H., Zhu, Y., Zhu, T., Liu, J. and Liu, W.: Investigations of  
709 temporal and spatial distribution of precursors SO<sub>2</sub> and NO<sub>2</sub> vertical columns in the North  
710 China Plain using mobile DOAS, *Atmos. Chem. Phys.*, 18, 1535–1554, doi:10.5194/acp-2017-  
711 719, 2017.
- 712 Wu, Z., Hu, M., Liu, S., Wehner, B., Bauer, S., Maßling, A., Wiedensohler, A., Petäjä, T., Dal  
713 Maso, M. and Kulmala, M.: New particle formation in Beijing, China: Statistical analysis of a  
714 1-year data set, *J. Geophys. Res.*, 112(D9), D09209, doi:10.1029/2006JD007406, 2007.
- 715 Xiao, S., Wang, M. Y., Yao, L., Kulmala, M., Zhou, B., Yang, X., Chen, J. M., Wang, D. F., Fu, Q.  
716 Y., Worsnop, D. R. and Wang, L.: Strong atmospheric new particle formation in winter in  
717 urban Shanghai, China, *Atmos. Chem. Phys.*, 15(4), 1769–1781, doi:10.5194/acp-15-1769-  
718 2015, 2015.
- 719 Yao, L., Garmash, O., Bianchi, F., Zheng, J., Yan, C., Kontkanen, J., Junninen, H., Mazon, S. B.,  
720 Ehn, M., Paasonen, P., Sipilä, M., Wang, M., Wang, X., Xiao, S., Chen, H., Lu, Y., Zhang, B.,  
721 Wang, D., Fu, Q., Geng, F., Li, L., Wang, H., Qiao, L., Yang, X., Chen, J., Kerminen, V.-M.,  
722 Petäjä, T., Worsnop, D. R., Kulmala, M. and Wang, L.: Atmospheric new particle formation  
723 from sulfuric acid and amines in a Chinese megacity, *Science*, 361(6399), 278–281,  
724 doi:10.1126/science.aao4839, 2018.
- 725 Yue, D., Hu, M., Wu, Z., Wang, Z., Guo, S., Wehner, B., Nowak, A., Achtert, P., Wiedensohler, A.,  
726 Jung, J., Kim, Y. J. and Liu, S.: Characteristics of aerosol size distributions and new particle  
727 formation in the summer in Beijing, *J. Geophys. Res. Atmos.*, 114(14), 1–13,  
728 doi:10.1029/2008JD010894, 2009.
- 729 Zhang, Y. M., Zhang, X. Y., Sun, J. Y., Lin, W. L., Gong, S. L., Shen, X. J. and Yang, S.:  
730 Characterization of new particle and secondary aerosol formation during summertime in  
731 Beijing, China, *Tellus, Ser. B Chem. Phys. Meteorol.*, 63(3), 382–394, doi:10.1111/j.1600-  
732 0889.2011.00533.x, 2011.
- 733 Zheng, J., Khalizov, A., Wang, L. and Zhang, R.: Atmospheric pressure-ion drift chemical  
734 ionization mass spectrometry for detection of trace gas species, *Anal. Chem.*, 82(17), 7302–  
735 7308, doi:10.1021/ac101253n, 2010.
- 736 Zheng, J., Hu, M., Zhang, R., Yue, D., Wang, Z., Guo, S., Li, X., Bohn, B., Shao, M., He, L., Huang,  
737 X., Wiedensohler, A. and Zhu, T.: Measurements of gaseous H<sub>2</sub>SO<sub>4</sub> by AP-ID-CIMS during  
738 CAREBeijing 2008 Campaign, *Atmos. Chem. Phys.*, 11(15), 7755–7765, doi:10.5194/acp-11-  
739 7755-2011, 2011.
- 740 Zheng, J., Yang, D., Ma, Y., Chen, M., Cheng, J., Li, S. and Wang, M.: Development of a new  
741 corona discharge based ion source for high resolution time-of-flight chemical ionization mass  
742 spectrometer to measure gaseous H<sub>2</sub>SO<sub>4</sub> and aerosol sulfate, *Atmos. Environ.*, 119, 167–173,  
743 doi:10.1016/j.atmosenv.2015.08.028, 2015.
- 744



Table 1 Mean, median, 5-95 % percentiles of key atmospheric variables and [H<sub>2</sub>SO<sub>4</sub>] in the daytime.

	UVB (W m <sup>-2</sup> )	[SO <sub>2</sub> ] (ppbv)	CS (s <sup>-1</sup> )	[O <sub>3</sub> ] (ppbv)	[HONO] (ppbv)	[NO <sub>2</sub> ] (ppbv)	[H <sub>2</sub> SO <sub>4</sub> ] (× 10 <sup>6</sup> molecule cm <sup>-3</sup> )	RH (%)
mean	0.17	4.6	0.11	10.5	0.74	25.3	5.4	28
median	0.14	3.7	0.11	9.0	0.51	23.0	4.9	26
5-95% percentiles	0.00-0.45	0.9-11.4	0.01-0.24	3.5-23.3	0.09-2.65	3.3-61.4	2.2-10.0	9-59



Table 2 Correlation coefficients (Spearman type) between [H<sub>2</sub>SO<sub>4</sub>] and atmospheric variables in the daytime. Only correlation coefficients with p-values less than 0.01 are included to ensure a statistical significance.

	UVB	[SO <sub>2</sub> ]	CS	[O <sub>3</sub> ]	[HONO]	[NO <sub>2</sub> ]	[H <sub>2</sub> SO <sub>4</sub> ]
UVB	1	/	/	0.14	-0.23	/	0.46
[SO <sub>2</sub> ]		1	0.83	0.25	0.64	0.70	0.74
CS			1	0.36	0.75	0.77	0.60
[O <sub>3</sub> ]				1	/	/	0.29
[HONO]					1	0.88	0.39
[NO <sub>2</sub> ]						1	0.53
[H <sub>2</sub> SO <sub>4</sub> ]							1





Table 3 Proxy functions for the nonlinear fitting procedure.

Proxy	Equation <sup>#</sup>
N1	$k_0 \cdot UVB^a \cdot [SO_2]^b \cdot CS^c$
N2	$k_0 \cdot UVB^a \cdot [SO_2]^b$
N3	$k_0 \cdot UVB^a \cdot [SO_2]^b \cdot CS^c \cdot [O_3]^d$
N4	$k_0 \cdot UVB^a \cdot [SO_2]^b \cdot [O_3]^d$
N5	$k_0 \cdot UVB^a \cdot [SO_2]^b \cdot CS^c \cdot ([O_3]^d + [HONO]^e)$
N6	$k_0 \cdot UVB^a \cdot [SO_2]^b \cdot ([O_3]^d + [HONO]^e)$
N7	$k_0 \cdot UVB^a \cdot [SO_2]^b \cdot CS^c \cdot ([O_3]^d + [NO_2]^f)$

<sup>#</sup>UVB is the intensity of ultraviolet radiation b in  $W\ cm^{-3}$ ;  $[SO_2]$  is the concentration of sulfur dioxide in molecule  $cm^{-3}$ ; CS is the condensation sink in  $s^{-1}$ ;  $[O_3]$  is the concentration of ozone in molecule  $cm^{-3}$ ; [HONO] is the concentration of nitrous acid in molecule  $cm^{-3}$ ;  $[NO_2]$  is the concentration of nitrogen dioxide in molecule  $cm^{-3}$ ;  $k_0$  is a scaling factor.



Table 4 Results of the nonlinear fitting procedure for different proxy functions, together with correlation coefficient ( $R$ , Pearson type) and mean absolute error ( $MAE$ ).

Proxy	$k_0$	$a$	$b$	$c$	$d$	$e$	$f$	$R$	$MAE (\times 10^6 \text{ molecule cm}^{-3})$
N1	515.74	0.14	0.38	0.03				0.83	1.03
N2	280.05	0.14	0.40					0.83	1.03
N3	9.95	0.13	0.39	-0.01	0.14			0.85	1.00
N4	14.38	0.13	0.38		0.14			0.85	1.00
N5	0.0072	0.15	0.41	-0.17	0.36	0.38		0.86	0.94
N6	2.38	0.14	0.33		0.24	0.24		0.85	0.98
N7	0.0013	0.13	0.40	-0.17	0.44		0.41	0.86	0.95



### Figure Captions

**Figure 1.** Correlations (a) between  $[\text{H}_2\text{SO}_4]$  and UVB intensity, and (b) between  $[\text{H}_2\text{SO}_4]$  and  $[\text{SO}_2]$ .  $k_m$  is a constant term.

**Figure 2.** Correlation between  $[\text{HONO}]$  and  $[\text{NO}_2]$ . The black line represents a linear fitting with a zero intercept.

**Figure 3.** Performance assessments of proxy N2 and proxy N7. The averaged deviation and the relative deviation in the plots are defined by Eq. (6) and Eq. (7) and used to evaluate the performance of proxy N2 and N7, respectively. “Overlap” refers to the smaller values between proxy N2 and proxy N7, and the larger ones are indicated by the color code of proxies N2 and N7.

**Figure 4.** Comparison of measured  $[\text{H}_2\text{SO}_4]$ ,  $[\text{H}_2\text{SO}_4]_{\text{N2}}$ ,  $[\text{H}_2\text{SO}_4]_{\text{N7}}$  and  $[\text{H}_2\text{SO}_4]_{\text{Petäjä et al.}}$  on 10 March, 2018 with a time resolution of 5 min.

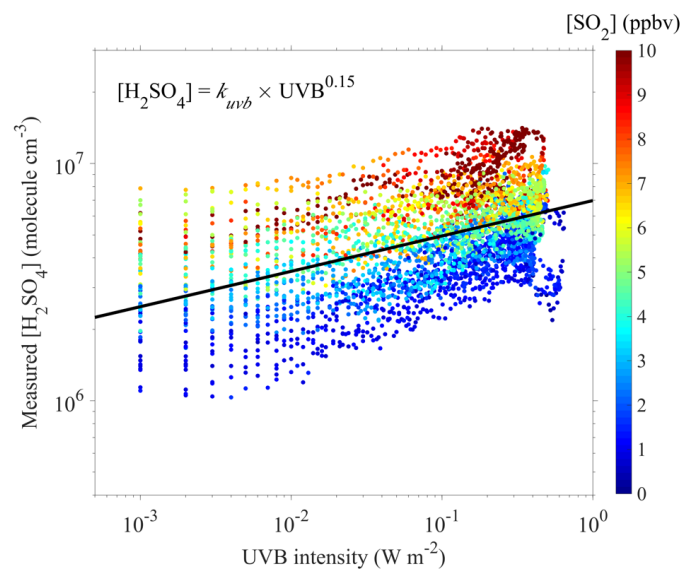


Figure 1a

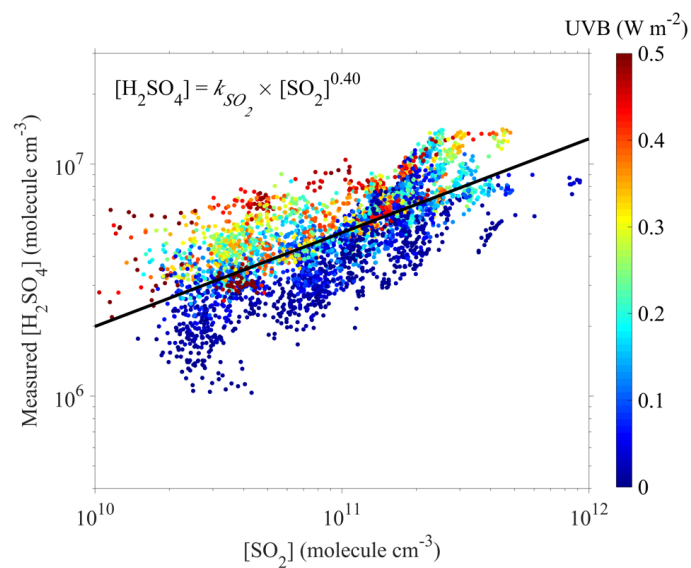
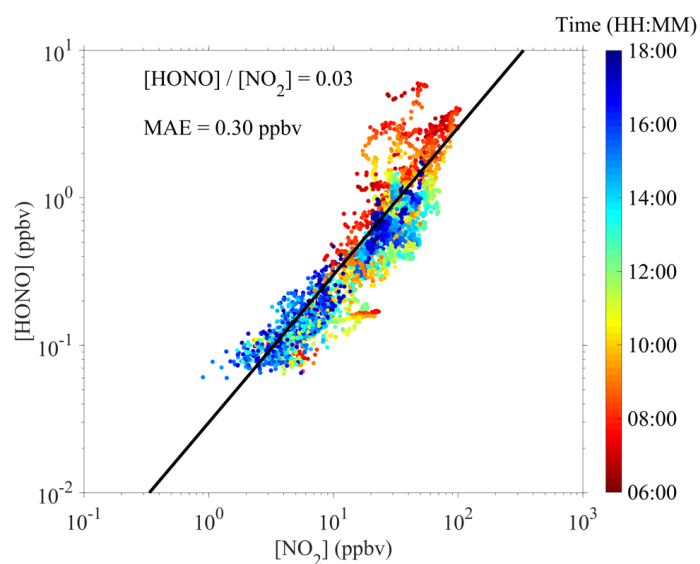


Figure 1b



**Figure 2**

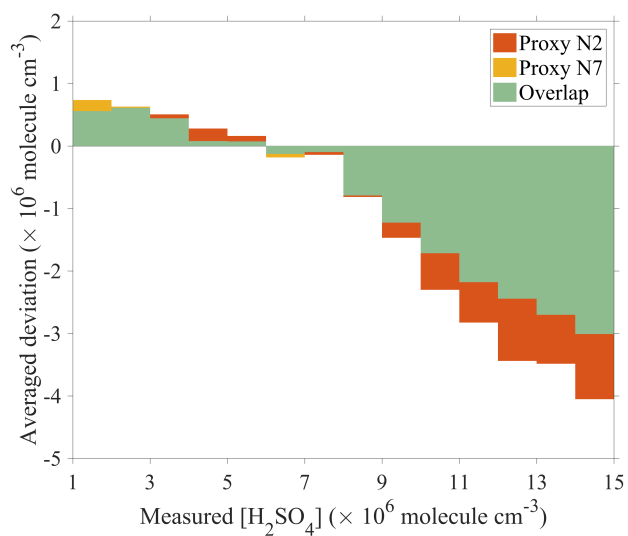


Figure 3a

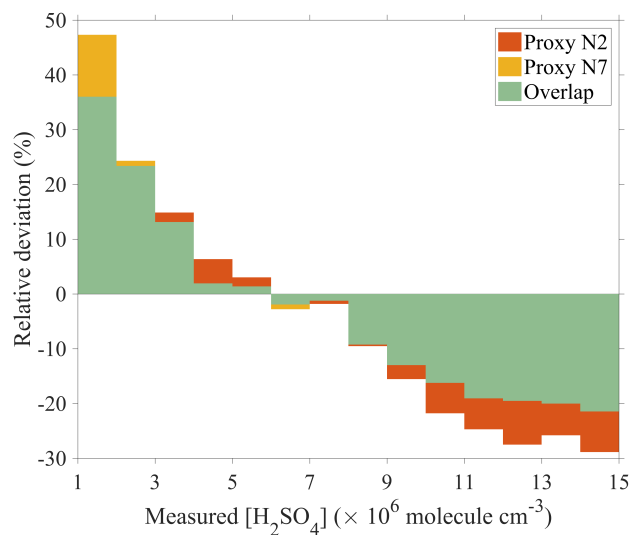


Figure 3b

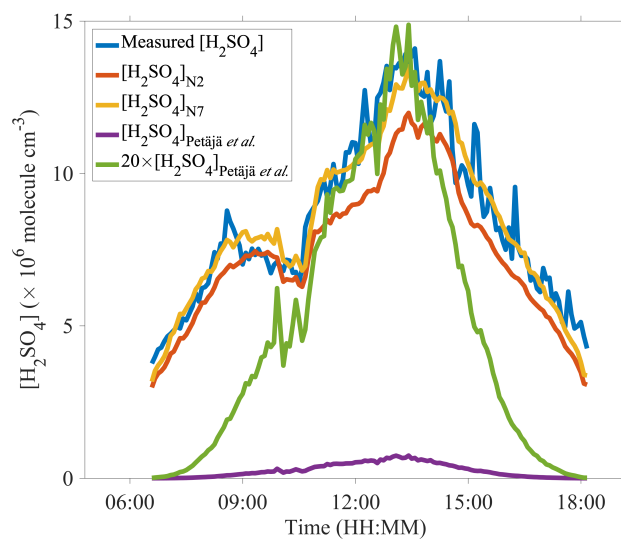


Figure 4